

# A Full-Wavelength Dipole RF Coil Element for 7 T MRI with Maximized Longitudinal FOV and Two-Peak SAR Distribution

A. Rennings<sup>1</sup>, A. Litinsky<sup>1</sup>, P. Schneider<sup>1</sup>, S. Orzada<sup>2</sup>, and S. Otto<sup>3</sup>

<sup>1</sup>General and Theoretical Electrical Engineering (ATE), Faculty of Engineering, University of Duisburg-Essen, 47048 Duisburg, Germany, <sup>2</sup>Erwin L. Hahn Institute for Magnetic Resonance Imaging, University of Duisburg-Essen, 45141 Essen, Germany, <sup>3</sup>High-Frequency Engineering (HFT), Faculty of Engineering, University of Duisburg-Essen, 47048 Duisburg, Germany

**INTRODUCTION:** Recently multi-channel RF coils based on several longitudinally oriented strip-line elements have been successfully applied in ultra-high field MRI. Among the different utilized strip-line approaches, the symmetrically fed dipole RF coil element initially presented in [1] which was terminated by two meander in [2, 3] seems to be one of the most promising candidates. This 25 cm long dipole element is slightly longer than half a wavelength (“ $\lambda/2$ -plus”) and is therefore not intrinsically eigen-resonant. In [4] the first homogeneous “from top to toe” MR image at 7 T has been scanned with the help of a whole-body coil array consisting of 16 of these meander elements. The authors took 28 successive overlapping scans, each with a longitudinal extend of approx. 25 cm. On the basis of this  $\lambda/2$ -plus-approach we developed a longitudinally extended coil element which exhibits a nearly full-wavelength resonant current distribution (“ $\lambda$ -minus”) with two distinct improvements – an RF field of view (FOV) that is maximized due to the longer extent and a lowered peak SAR<sub>10g</sub> due to a more appropriate two-peak electric field distribution.

**MATERIALS and METHODS:** Compared to the initial design where a 2 cm thick PMMA block together with copper foil for the metallization was used [2] the material stack is slightly changed. The  $\lambda$ -minus strip-line element and the corresponding metal plate used for shielding purposes are printed on low cost FR-4 substrates ( $\epsilon_r \approx 4.4$ ,  $\tan(\delta) \approx 0.02$ ) with a thickness of 0.5 mm. These printed circuit boards (PCBs) are separated by 20 mm of air. The distance can be controlled / adjusted via six polyamide screws along the edge of the PCBs. The influence of loading is considered by using a flat phantom 20 mm separated from the top PCB. Its material parameters are  $\epsilon_r = 40$  and  $\sigma = 0.8$  S/m in order to emulate the human body in the frequency range around 300 MHz. The lateral dimensions of the two PCBs are 450 mm in length and 100 mm in width. The width of the metallic strip-line is 15 mm and the geometry of the meanders remains unchanged in comparison to [2]. This is also true for the end-capacitor with a value of  $C_{end} = 1$  pF, but not for the matching/tuning network including a balun symmetrically located at the backside of the ground plane. For the proposed  $\lambda$ -minus strip-line a simplified matching network with only one capacitor can be used, in contrast to the shorter  $\lambda/2$ -plus element of [1, 2] where altogether three capacitors were needed. This aspect is further elaborated in the following section. The numerical evaluations were carried out with the FDTD software EMPIRE Xcel (IMST GmbH, Kamp-Lintfort, Germany).

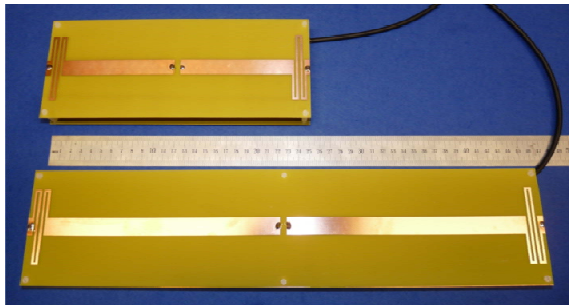


**Fig. 1:** Prototypes of the  $\lambda/2$ -plus-element (top, 25 cm long) and the  $\lambda$ -minus-strip-line (bottom, 45 cm long) -- for both a return loss of 25 dB has been measured.

**RESULTS and DISCUSSION:** The already mentioned simplified matching network is based on the special complex input impedance  $Z_{\lambda\text{-minus}}(\omega_0) = R(\omega_0) + jX(\omega_0)$  of the intrinsic  $\lambda$ -minus-element. Since the proposed dipole element is slightly shorter than the required length for a full-wavelength high-impedance anti-resonance operation it can be matched to  $50 \Omega$  by applying just one series capacitor (cf. Fig. 2). In this case the length of the  $\lambda$ -minus-strip-line must be adjusted so that  $R(\omega_0) \approx 50 \Omega$ . The FDTD simulations predicted a value of 2.4 pF for  $C_{sc}$ . In practice it might be better to have more than one degree of freedom for adjusting the matching and the frequency tuning. The excited fields inside the flat phantom (6 cm above the top PCB) of the  $\lambda$ -minus and the  $\lambda/2$ -plus strip-line element are now compared and discussed. The fields only 1 cm above the top PCB – so the field between top PCB and phantom – are also shown, but are not further discussed, due to a lack of interest for the MRI application. The comparison is carried out as fair as possible. Therefore the accepted input power was equal to 12.4 W for both FDTD simulations. This is due to a 1-Ampere FDTD current source with  $50 \Omega$  lumped port impedance. Furthermore the flat phantom has the same dimensions for both cases. The magnetic field component plots in Fig. 3 and Fig. 4 indicate two important results: The FOV with adequate RF magnetic field of the  $\lambda$ -minus-element reaches 45 cm and matches quite well the 50 cm diameter of the spherical volume with homogeneous static field of the used 7 T whole-body MR system (Magnetom 7T, Siemens, Erlangen) and is nearly twice as long as for the  $\lambda/2$ -plus-element. In this case the aforementioned from-top-to-toe MRIs can be accomplished by a minimum of longitudinally shifted single scans. Thus the quite expensive scanner time is minimized. On the other hand the  $B_1$ -efficiency is only slightly lower for the extended element (1.2 A/m vs. 1.4 A/m for  $\max[H_y(h = 6 \text{ cm})]$ ). Another important observation can be made in Figs. 5 and 6. It corresponds to a lowered SAR<sub>10g</sub> peak value of the  $\lambda$ -minus-element compared to more conventional strip-line elements with a length of less than  $3/4$  of  $\lambda$  where the SAR<sub>10g</sub> distribution exhibits only one maximum located at the lateral centre, as depicted in Fig. 6 for the  $\lambda/2$ -plus-strip-line. In contrast the new element exhibits two maxima along the longitudinal direction (cf. Fig. 5). The RF power that is dissipated in the human body during the MRI scan is therefore better distributed in the later case (2.6 mW/g vs. 3.8 mW/g for  $\max[SAR_{10g}(h = 6 \text{ cm})]$ ). It is expected that the novel  $\lambda$ -minus strip-line element allows a higher excitation voltage, since the local SAR, and not the global whole-body SAR, is usually the limiting value for ultra-high field MRI excitations. Our future research will focus on coupling investigations for the novel  $\lambda$ -minus strip-line element and initial evaluations in a 7 T whole-body MRI scanner.

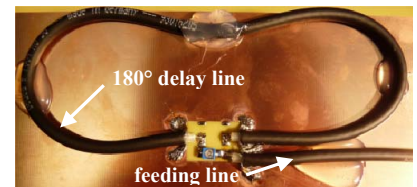


**Fig. 2:** On the backside of the bottom PCB the balun with a 180° delay coaxial cable and the matching network with only one series capacitor  $C_{sc} \approx 2.4$  pF is located.

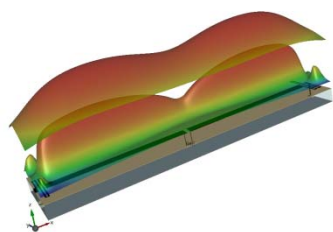


**Fig. 3:**  $H_y(x, y, h)$  for the 45 cm element at 300 MHz; lower plot in air with  $\max[H_y(h = 1 \text{ cm})] = 9.32$  A/m; upper plot inside the phantom with  $\max[H_y(h = 6 \text{ cm})] = 1.22$  A/m;

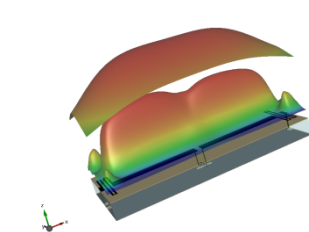


**Fig. 4:**  $H_y(x, y, h)$  for the 25 cm element at 300 MHz; lower plot in air with  $\max[H_y(h = 1 \text{ cm})] = 12.24$  A/m; upper plot inside the phantom with  $\max[H_y(h = 6 \text{ cm})] = 1.43$  A/m;

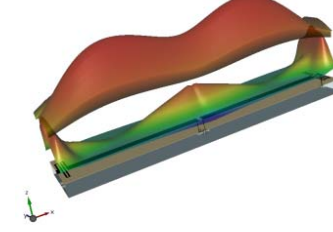


**Fig. 5:** E-fields( $x, y, h$ ) for the 45 cm element; lower plot in air with  $\max[|E|(h = 1 \text{ cm})] = 5700$  V/m, upper plot inside the phantom with  $\max[SAR_{10g}(h = 6 \text{ cm})] = 2.64$  mW/g;

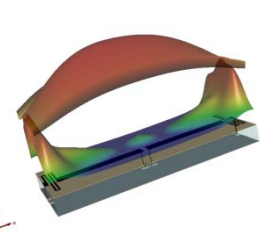


**Fig. 6:** E-fields( $x, y, h$ ) for the 25 cm element; lower plot in air with  $\max[|E|(h = 1 \text{ cm})] = 7780$  V/m, upper plot inside the phantom with  $\max[SAR_{10g}(h = 6 \text{ cm})] = 3.79$  mW/g;

**REFERENCES:** [1] D. O. Brunner et al., Proc. Intl. Soc. MRM 15 (2007). [2] S. Orzada et al., Proc. Intl. Soc. MRM 16 (2008), 2979. [3] A. Bahr, German Patent Application DE102007053483A1. [4] S. Orzada et al., Proc. Intl. Soc. MRM 18 (2010), 50.